

Intracranial embryonal neoplasm in an alpaca

Journal of Veterinary Diagnostic Investigation
2023, Vol. 35(6) 777–781
© 2023 The Author(s)
Article reuse guidelines:
sagepub.com/journals-permissions
DOI: 10.1177/10406387231195611
jvdi.sagepub.com

Alexandra Fielding, Jillian Minuto, Melissa Mazan,
Andrew D. Miller,  Shelley J. Newman¹ 

Abstract. An 11-y-old hembra alpaca was admitted because of cerebellar and vestibular signs, dysphagia, and aspiration pneumonia; without clinical improvement following empirical therapy, the patient was euthanized. On autopsy, a neoplasm was found incorporating the right vestibulocochlear nerve at the level of the acoustic meatus. Histologically, the mass was composed of a multiphasic primitive cell population associated with a dense fibrous stroma and enveloping a remnant ganglion and nerve bundles. Patterns included dense ribbons and cords of embryonal neuroepithelial cells admixed with loosely defined interlacing spindle cells. The embryonal cells had angular cell profiles with variable amounts of lightly basophilic cytoplasm, ovoid-to-irregular nuclei, and an open chromatin pattern with a typically inapparent nucleolus. Necrosis was not evident, and there was 1 mitotic figure per 2.37 mm². The entire mass was infiltrated by small numbers of lymphocytes and plasma cells. Immunohistochemistry (IHC) revealed strong and diffuse cytoplasmic immunolabeling for vimentin, microtubule-associated protein-2, protein gene product 9.5, and synaptophysin; ~50% immunolabeling for cytokeratin AE1/3; sporadic OLIG2 and S100 immunolabeling; and absent glial fibrillary acidic protein immunolabeling. Based on the histologic pattern and the IHC results, our diagnosis was a poorly differentiated embryonal tumor with ependymal differentiation associated with the vestibulocochlear nerve.

Keywords: camelids; germ cell and embryonal; immunohistochemistry; neoplasms; New World camelids.

Embryonal tumors are neoplasms that arise from the germinal neuroectoderm of the developing nervous system and can differentiate along several cell lines.¹¹ Embryonal CNS tumor categorization has evolved significantly since its first description in 1959.⁵ Historically, the term *primitive neuroectodermal tumor* (PNET) was applied only to supratentorial embryonal tumors, but given their resemblance to cerebellar medulloblastomas, the PNET category was expanded to include all embryonal tumors in the CNS and function as an umbrella category for primitive tumors that lacked differentiating features. Although the term PNET is no longer widely used in human medicine, the number of tumors included under this category has grown as a result of advancements in histologic, genetic, and molecular characterizations. In the human WHO classification system, these neoplasms have been separated into 2 groups by using morphologic and molecular features of the cell lines of origin: 1) medulloblastomas and 2) other embryonal tumors, the latter being a broader category that includes embryonal tumors with multilayered rosettes, neuroblastomas, ganglioneuroblastomas, medulloepitheliomas, ependymoblastomas, atypical teratoid/rhabdoid tumors, and poorly differentiated embryonal tumors.^{13–15}

Medulloblastomas, which make up most embryonal tumors, are found primarily in the cerebellar hemispheres or dorsal brainstem.^{11,17,19} They appear to be most common in

calves, with rare occurrences reported in adult cats, pigs, dogs, rats, non-human primates, a grizzly bear, and a kowari.^{11,17} There are a few reports of non-medulloblastoma embryonal tumors within the CNS in veterinary species, but reports suggest they are most common in the supratentorial region and less so in the spinal cord, nerves, and ganglia.^{7,10,16,17} Additionally, non-medulloblastoma embryonal tumors can occur peripherally in bone or soft tissue, and there have been a number of veterinary case reports of intracranial embryonal tumors, including 3 instances in llamas.¹⁶

The prevalence of neoplasia or proliferative lesions in New World camelids is estimated at 7–9% of all New World camelid autopsy submissions.^{1,20} The most common types of neoplasia reported in New World camelids are lymphoma and cutaneous or mucocutaneous fibroma or fibropapilloma; tumors within the cranial cavity have been described only rarely.^{1,19} The few exceptions include an intracranial teratoma in an alpaca,¹² a gemistocytic astrocytoma in a llama,⁸

Hospital for Large Animals, Cummings School of Veterinary Medicine, Tufts University, North Grafton, MA, USA (Fielding, Minuto, Mazan); College of Veterinary Medicine, Cornell University, Ithaca, NY, USA, USA (Miller); Newman Specialty VetPath, Hicksville, NY, USA (Newman).

¹Corresponding author: Shelley J. Newman, Newman Specialty VetPath, 19 Gables Dr, Hicksville, NY 11801, USA. pathvet3@gmail.com

a pituitary adenoma in an alpaca,⁹ and a pituitary null cell adenoma in a llama.³ Here we describe the clinical presentation, autopsy findings, and histopathology of an intracranial embryonal neoplasm in an alpaca with myriad clinical signs, including neurologic deficits attributable to the mass.

An 11-y-old hembra alpaca (*Vicugna pacos*) was referred to the Hospital for Large Animals at the Cummings School of Veterinary Medicine at Tufts University (North Grafton, MA, USA) following a 2-wk history of neurologic abnormalities including dysphagia, cerebellar and vestibular signs, and suspected aspiration pneumonia. Clinical examination revealed normal vital parameters and auscultation, but malodorous nasal discharge was present bilaterally. On neurologic assessment, the patient was quiet but hyperesthetic to touch and noise stimulation, and circled to the right. Further neurologic assessment revealed a head tilt to the right, right-sided facial nerve paralysis demonstrated by an inability to blink and decreased flare of the right nostril, hypermetria in both hindlimbs, broad-based stance of the hindlimbs, and a lean to the right. Because of the lack of a blink reflex, fluorescein stain was applied to the right eye, and a superficial corneal ulcer was identified.

Hematologic examination and clinical chemistry revealed minor alterations, none of which were considered relevant to the neurologic presentation. Radiographs of the cervical and thoracic spine revealed no abnormalities; a mild bronchointerstitial infiltrate was noted caudal to the heart. A lumbosacral CSF sample was within normal limits: colorless, clear, 282 g/L protein (RI: <500 g/L), total nucleated cell count of 9 (mononuclear predominant), with no eosinophils or infectious organisms observed.

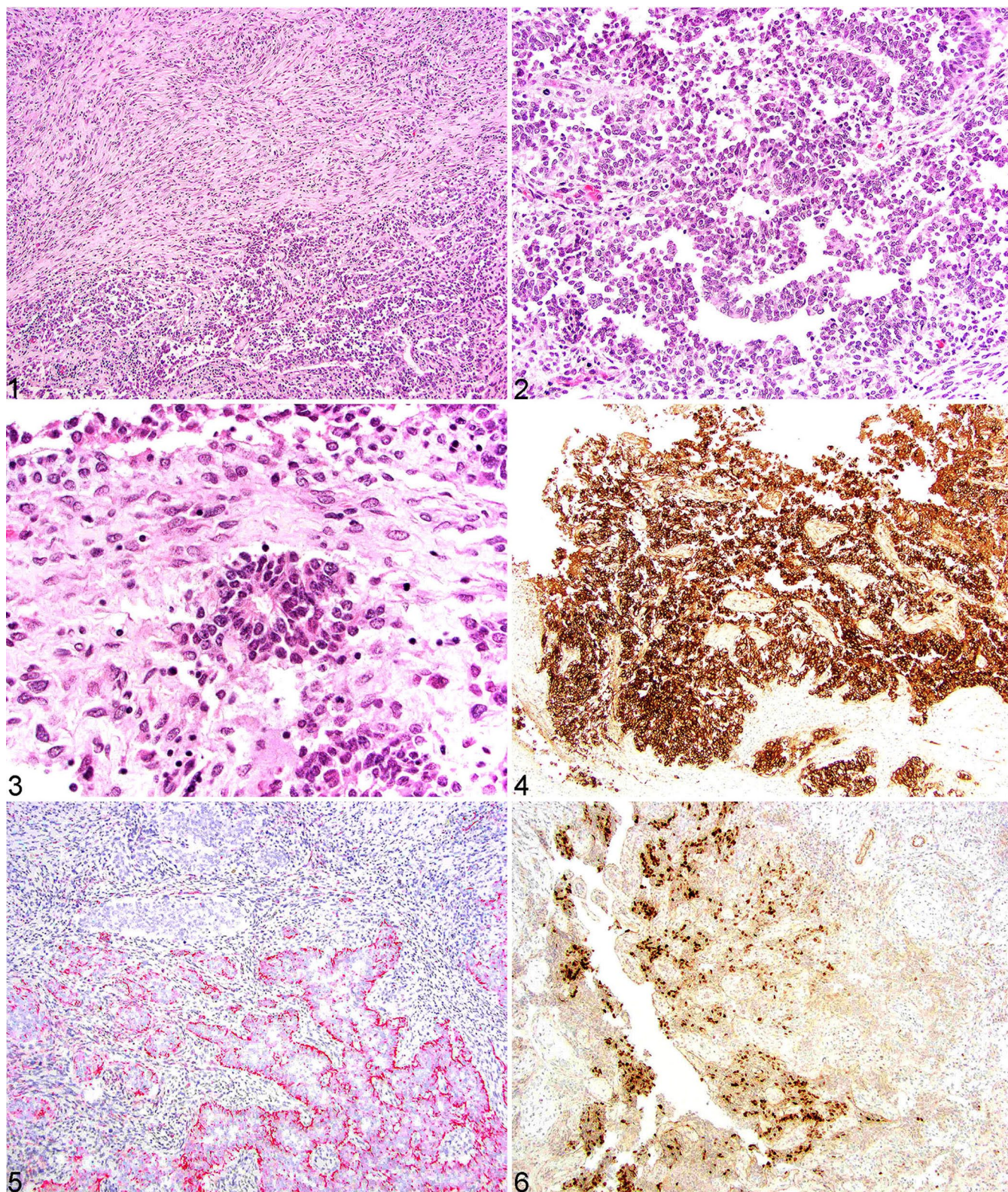
Based on the history, physical examination, and initial testing, primary neurologic disease was suspected with concurrent secondary respiratory changes. Space-occupying lesions (e.g., neoplasm, granuloma, abscess), parasitic migration (e.g., *Parelaphostrongylus tenuis*), otitis media and/or interna, and listeriosis were the primary differential diagnoses. Initial therapy based on the clinical differentials included supportive and ulcer-specific medications.

Because of marked worsening of clinical signs over the next 4 d, euthanasia was elected, and an autopsy was performed ~24 h following euthanasia. At autopsy, the following lesions were identified: right corneal ulcer, bronchopneumonia, gastric ulcers, and fibrinonecrotizing colitis. Examination of the brain revealed a 2 × 2 × 0.8-cm tan, soft mass extending from the opening of the vestibulocochlear canal and incorporating the vestibulocochlear nerve, compressing the right ventral side of the brainstem. The spinal cord was not assessed at autopsy. Routine sections of all major organs and the brain mass were fixed in 10% neutral-buffered formalin, processed routinely into paraffin blocks, sectioned at 4 μm, and stained with H&E. Additional histochemical stains (periodic acid–Schiff [PAS] and phosphotungstic acid–hematoxylin [PTAH]) were performed according to standard laboratory procedures.

Histologically, the mass affected the region of the acoustic meatus and incarcerated adjacent ganglia and soft tissue. The mass was composed of primitive embryonal neoplastic cells associated with remnant ganglion cells and bundles of pre-existent nerve present around the perimeter of the mass, but not part of the mass proper. Most of the neoplastic cells formed cords, ribbons, nests, and rosettes supported by a moderate neuropil-like parenchyma (Figs. 1, 2). The rosettes (Flexner–Wintersteiner) had a periphery of neuroblastic cells (single layer) and a mostly empty central lumen into which small cytoplasmic processes protruded (Fig. 3). These cells were round-to-angular-to-elongate with variable amounts of lightly basophilic cytoplasm, deeply basophilic nuclei, and finely stippled chromatin. Occasional faint cytoplasmic processes extended from the apical portion of the neoplastic cells. Atypia was moderate, and the mitotic count was 1 mitotic figure in 10 hpfs (2.37 mm²). No necrosis was observed in the mass, yet it was infiltrated by small numbers of lymphocytes and plasma cells. No PAS- or PTAH-positive material was detected in the neoplastic cells. Additional comorbid histology findings included: aspiration pneumonia, ulcerative lesions in C1–C3, fibrinous peritonitis, and fibrinonecrotizing colitis.

Formalin-fixed, paraffin-embedded neoplastic tissues were processed for immunohistochemistry (IHC) using the following antibodies (Table 1): protein gene product 9.5 (PGP9.5); synaptophysin (SYN); cytokeratin AE1/AE3 (CKAE1/AE3); oligodendrocyte transcription factor 2 (OLIG2); glial fibrillary acidic protein (GFAP); microtubule-associated protein 2 (MAP2); S100; and vimentin. All antibody studies were performed on an automated Leica Bond-Max system. For all antibodies, glass-mounted paraffin scrolls were dewaxed (Bond dewax solution; Leica), followed by heat epitope retrieval and antibody application (Table 1). Following antibody application, the Leica Bond polymer detection kit was applied for 20 min (SYN, GFAP, S100) or 40 min (PGP9.5, OLIG2). CKAE1/AE3, MAP2, and vimentin had PolyVision Poly-HRP anti-mouse IgG reagent (Leica) added for 30 min followed by Leica Bond polymer refine red detection kit for 10 min (MAP2, vimentin) or 15 min (CKAE1/AE3). All IHC slides were counterstained with hematoxylin for 5 min.

IHC staining revealed robust, diffuse, cytoplasmic immunolabeling for vimentin. Less than 15% of the neoplastic cells had strong cytoplasmic labeling for S100; however, S100 highlighted the surrounding nerve bundles and incarcerated remnant nerves within the mass (internal control). Robust cytoplasmic immunolabeling was present diffusely in the neoplastic cells for MAP2 (Fig. 4), PGP9.5, and SYN. Both PGP9.5 and SYN also extensively labeled the adjacent nerve (internal control). Approximately 50% of the neoplastic cells had strong, cytoplasmic, often apical immunolabeling for CKAE1/AE3 (pan-cytokeratin; Fig. 5). Approximately 5% of the neoplastic cells had strong intranuclear immunolabeling



Figures 1–6. CNS embryonal tumor in an alpaca. **Figure 1.** Some areas of the neoplasm had neoplastic cells arranged in interlacing streams and bundles adjacent to the more primitive cells arranged in ribbons and cords. H&E. **Figure 2.** Primitive neoplastic cells are arranged in ribbons and cords with lightly basophilic cytoplasm with large round-to-ovoid nuclei, finely stippled chromatin, and inapparent nucleoli. H&E. **Figure 3.** Scattered throughout the neoplasm are Flexner–Wintersteiner rosettes typified by fine fibrillary processes in the rosette lumen. H&E. **Figure 4.** Neoplastic cells had strong and diffuse cytoplasmic MAP2 immunolabeling. **Figure 5.** Approximately 50% of the neoplastic cells had strong cytoplasmic, often apical, cytokeratin AE1/AE3 immunolabeling. **Figure 6.** Less than 10% of the neoplastic cells had strong intranuclear OLIG2 immunolabeling.

Table 1. Antibodies with source, clone, concentration used, retrieval information, and detection method.

Antibody	Host	Source	Clone	Antigen retrieval	Dilution	Positive camelid control
PGP9.5	Rabbit	Agilent	Z511601	Heat*	1:1000	Brain
SYN	Rabbit	Abcam	Ab14692	Heat†	1:100	Brain
CKAE1/AE3	Mouse	Agilent	B3515	Heat*	1:200	Intestine
OLIG2	Rabbit	Abcam	Ab109186	Heat‡	1:2000	Brain
GFAP	Rabbit	Agilent	Z0334	None	1:5000	Brain
MAP2	Mouse	Sigma-Aldrich	45-M4403	Heat†	1:1000	Brain
S100	Rabbit	Agilent	Z0311	None	1:400	Brain
Vimentin	Mouse	Agilent	M7020	Heat§	1:80	Intestine

CKAE1/AE3=cytokeratin AE1/AE3; GFAP=glial fibrillary acidic protein; MAP2=microtubule-associated protein 2; OLIG2=oligodendrocyte transcription factor 2; PGP9.5=protein gene product 9.5; SYN=synaptophysin.

* Heat retrieval for 20 min (Bond epitope retrieval solution 1; Leica).

† Heat retrieval for 30 min (Bond epitope retrieval solution 1; Leica).

‡ Heat retrieval for 30 min (Bond epitope retrieval solution 2; Leica).

§ Heat retrieval for 10 min (Bond epitope retrieval solution 1; Leica).

for OLIG2 (Fig. 6). Neoplastic cells lacked immunolabeling for GFAP.

Given the lack of distinctive morphologic features and unique molecular findings, diagnosis of embryonal tumors involves assessment of a range of factors, including anatomic location, histologic features, and IHC.^{10,17} The histologic pattern and cellular morphology can be wide-ranging because embryonal tumors have various degrees of neural differentiation.¹⁶ In our case, the mass involved primitive, or poorly differentiated, embryonal cells arranged primarily in rows, cords, and rosettes. Rosettes can be found in a variety of neural tumors including embryonal and ependymal tumors; however, the latter is considered less likely given the anatomic location in our case.^{14,19,21} Embryonal tumors of the nervous system can be broadly divided into central and peripheral, with similar histologic features present regardless of location. Although our case arose intracranially, it arose adjacent to the brain, and the specific site of origin could not be determined adequately.

Grossly, the neoplastic lesion in our case arose in an uncommon location for an embryonal tumor, extending from the vestibulocochlear canal and involving primarily the vestibulocochlear nerve. Because of the location of this lesion, several neurologic structures and their pathways and functions were affected: the facial and vestibulocochlear nerves, the medulla oblongata, and the cerebellum. Normally, the flow of impulses from the inner ear to the vestibular system allows for the coordination of eye, neck, trunk, and limb position with respect to the position and movement of the head. Although the tumor itself disrupted the vestibular pathway, the mass also caused compression of the medulla oblongata and cerebellum. Hence, the neurologic assessment of our patient revealed both peripheral and central vestibular signs, with the former including circling and head tilt to the side of the lesion (right), and the latter including decreased mentation and variable nystagmus.^{2,6} Furthermore, compression of the cerebellum caused classic cerebellar signs, such

as the patient's hypermetria and wide-based stance. The observed facial nerve paralysis is explained by damage to cranial nerve VII, which runs alongside cranial nerve VIII for much of its course.

The final challenge in confirming a diagnosis of an embryonal CNS tumor is that no single IHC stain is diagnostic, and a number of staining results have been described and reported given the various degrees of differentiation.^{4,7,10,16} Furthermore, the undifferentiated cells can branch into different lineages before phenotypic differentiation has occurred.¹⁶ In our case, the combination of positivity for conventional neuronal (SYN, MAP2, PGP9.5) and epithelial (CKAE1/AE3) neuroectodermal markers, as well as the histologic characteristics, point toward our final diagnosis of an embryonal CNS tumor with potential ependymal differentiation.¹⁸ The use of molecular testing to type embryonal tumors, such as chromosome 19 microRNA cluster (*C19MC*), or less commonly *DICER1*, as described by the World Health Organization Classification of Tumors of the Central Nervous System, have not been studied in veterinary species, to our knowledge.^{5,14,15}

Given the complexity and variability of the histologic and molecular characteristics of embryonal neoplasms, all relevant information must be taken into consideration to effectively communicate a tumor's characteristics and appropriately categorize it into a specific diagnosis when possible. The morphologic, histologic, and IHC findings of the neoplasm in our case are consistent with a poorly differentiated embryonal CNS tumor with ependymal differentiation, which adds to the differentials for primary intracranial neoplasia in alpacas.

Acknowledgments

We thank the members of the Tufts University Anatomic Pathology Department and the histology technicians at the Cornell University Animal Health Diagnostic Center Anatomic Pathology Laboratory.

Declaration of conflicting interests


The authors declared no potential conflicts of interest with respect to the research, authorship, and/or publication of this article.

Funding

The authors received no financial support for the research, authorship, and/or publication of this article.

ORCID iDs

Andrew D. Miller  <https://orcid.org/0000-0001-6350-5581>

Shelley J. Newman  <https://orcid.org/0000-0002-3471-4816>

References

1. Aboellail TA, et al. Neoplasia and proliferative lesions of new world camelids: a systematic literature review and retrospective study of cases submitted to Colorado State University from 1995 to 2020. *Front Vet Sci* 2021;8:743498.
2. Bedenice D, Whitehead C. A systematic approach to the neurological examination of llamas and alpacas. *Livestock* 2016;21:308–313.
3. Chalkley MD, et al. Pituitary null cell adenoma in a domestic llama (*Lama glama*). *J Comp Pathol* 2014;151:51–56.
4. Choi US, et al. Cytologic and immunohistochemical characterization of a primitive neuroectodermal tumor in the brain of a dog. *Vet Clin Pathol* 2012;41:153–157.
5. Cotter JA, Judkins AR. Evaluation and diagnosis of central nervous system embryonal tumors (non-medulloblastoma). *Pediatr Dev Pathol* 2022;25:34–45.
6. de Lahunta A, et al. The neurologic examination. In: de Lahunta A, et al., eds. *De Lahunta's Veterinary Neuroanatomy and Clinical Neurology*. 5th ed. Elsevier, 2021:531–546.
7. Gains MJ, et al. A primitive neuroectodermal tumor with extension into the cranial vault in a dog. *Can Vet J* 2011;52:1232–1236.
8. Garlick DS, et al. Gemistocytic astrocytoma in a one-month-old llama. *J Am Vet Med Assoc* 1990;196:2009–2010.
9. Gilsenan WF, et al. Neurologic disease attributed to a pituitary adenoma in an alpaca. *J Vet Intern Med* 2012;26:1073–1077.
10. Headley SA, et al. Central primitive neuroectodermal tumour with ependymal differentiation in a dog. *J Comp Pathol* 2009;140:80–83.
11. Higgins RJ, et al. Tumors of the nervous system. In: Meuten DJ, ed. *Tumors in Domestic Animals*. 5th ed. Wiley, 2017: 860–862.
12. Hill FI, Mirams CH. Intracranial teratoma in an alpaca (*Vicugna pacos*) in New Zealand. *Vet Rec* 2008;162:188–189.
13. Louis DN, et al. The 2007 WHO classification of tumours of the central nervous system. *Acta Neuropathol* 2007;114:97–109.
14. Louis DN, et al. The 2016 World Health Organization Classification of Tumors of the Central Nervous System: a summary. *Acta Neuropathol* 2016;131:803–820.
15. Louis DN, et al. The 2021 WHO Classification of Tumors of the Central Nervous System: a summary. *Neuro Oncol* 2021;23:1231–1251.
16. Martins BC, et al. Retrobulbar embryonal tumor with multilayered rosettes in a golden retriever dog. *Clin Case Rep* 2020;9:660–668.
17. McHale B, et al. Embryonal central nervous system tumor in the brain of a goose. *J Vet Diagn Invest* 2019;31:385–389.
18. Miller AD, et al. Canine ependymoma: diagnostic criteria and common pitfalls. *Vet Pathol* 2019;56:860–867.
19. Stoyanov GS, et al. A practical approach to the differential diagnosis of intracranial tumors: gross, histology, and immunoprofile-based algorithm. *Cureus* 2019;11:e6384.
20. Valentine BA, Martin JM. Prevalence of neoplasia in llamas and alpacas (Oregon State University, 2001–2006). *J Vet Diagn Invest* 2007;19:202–204.
21. Wippold FJ 2nd, Perry A. Neuropathology for the neuro-radiologist: rosettes and pseudorosettes. *Am J Neuroradiol* 2006;27:488–492.